High-pressure x-ray-absorption study of GaSe

J. Pellicer-Porres,* A. Segura, Ch. Ferrer, and V. Muñoz
Institut de Ciència dels Materials, Universitat de València, C\Dr. Moliner 50, Ed. Investigació, E-46100 Burjassot (València), Spain

A. San Miguel
Département de Physique des Matériaux, Bâtiment 203, Université Lyon I, 43 Bd. du 11 Novembre 1918, F-69622, Villeurbanne, France

A. Polian, J. P. Itié, and M. Gauthier
Physique des Milieux Condensés, CNRS-UMR 7602, Université Paris VI, 4 place Jussieu, F-75252 Paris Cedex 05, France

S. Pascarelli
European Synchrotron Radiation Facility, BP 220, 38043 Grenoble Cedex, France

(Received 30 April 2001; revised manuscript received 25 July 2001; published 16 April 2002)

We performed two x-ray-absorption experiments under pressure in GaSe, at the Ga and Se *K* edges (10.368 and 12.653 keV, respectively), up to 34 GPa. The Ga-Se distance obtained from the extended x-ray-absorption fine-structure fit decreases monotonically up to 16 ± 2 GPa, following a first-order Murnaghan equation of state with $B_0=92\pm6$ GPa and B_0' fixed to 5. Under a plausible hypothesis, we calculate the evolution of the whole structure up to 16 ± 2 GPa. These calculations indicate that the layer thickness decreases slightly under pressure.

DOI: 10.1103/PhysRevB.65.174103 PACS number(s): 61.10.Ht, 64.30.+t, 64.70.−p

I. INTRODUCTION

The III-VI layered family of semiconductors has attracted the interest of both theoretical and experimental researchers due to the presence of interactions of very different natures and for their potential applications. The most characteristic feature of this family of semiconductors is the existence of layers where bonds are covalent with a certain ionic component. Layers are held together by weak van der Waals forces. The properties of III-VI layered compounds in ambient conditions show a highly anisotropic behavior. Many technical applications have been proposed in the fields of solar cells,[1–3] nonlinear optics,[4–8] or as candidates for solid-state batteries.[9–11]

As a result of the very different natures of interactions in these materials, basic properties such as the unit-cell volume or the band gap show a markedly nonlinear behavior under pressure. Theoretical models able to describe not only the highly anisotropic physical properties at ambient pressure, but also to model their behavior under high pressure, constitute a challenging enterprise for solid state scientists.

GaSe belongs to the family of III-VI layered compounds. One layer may be viewed (Fig. 1) as formed by two cation-anion hexagonal cycles with a chairlike deformation, linked by strong Ga-Ga bonds. These bonds are perpendicular to the layer plane. Hence the Ga atoms are surrounded by three Se atoms and one Ga atom, whereas the Se atoms have three Ga first neighbors. On average, the Hume-Rothery rule is preserved. Stacking of the layers ensure compact packing of the anions, and gives rise to several stacking patterns, so-called polytypes. Depending on the growth method, GaSe has been found in β,[12] ε,[13–16] γ,[14,17] or δ (Ref. 18) polytypes. Bridgman grown samples are commonly found to follow the ε stacking pattern, with symmetry $P\bar{6}m2$ (D_{3h}^1) and a hexagonal unit cell described by $a=3.743$ Å and $c=15.919$ Å.

The ambient pressure properties of GaSe have been extensively studied. Under pressure, various types of experiments have been carried out: optical absorption,[19–22] reflectivity,[23] microphotographs,[19] ultrasonic,[24] transport,[25]

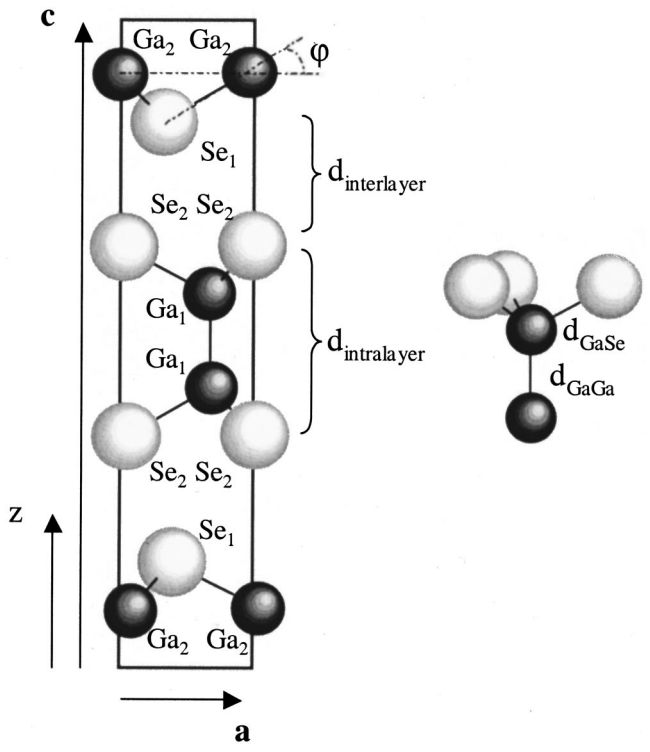

FIG. 1. Left: ε-GaSe unit cell as seen from the [010] direction. $d_{\text{intralayer}}$ and $d_{\text{interlayer}}$ represent the intralayer and interlayer distances, respectively. φ is the angle between the layer and the Ga-Se bond. Right: bond configuration detail. d_{GaGa} and d_{GaSe} refer, respectively, to the Ga-Ga and Ga-Se bond lengths.

resistance,[26] dielectric constant[19,27–29] and Raman spectroscopy.[19,30] An essential problem in the description of the physical properties at high pressure in III-VI layered compounds is the lack of information concerning the pressure evolution of the atomic positions inside the unit cell. In an x-ray diffraction (XRD) experiment information about the atomic positions is obtained through an analysis of the diffracted intensities. In III-VI layered semiconductors the presence of stacking faults or twinned planes makes it very difficult to obtain a pure single-crystalline sample. On the other hand, the layered character of the samples is such that every grain is a platelet which orientates parallel to the other as soon as pressure is applied, introducing preferential orientation in the powder. Consequently, the information coming from the intensity in a XRD experiment carried out in these materials is very difficult to extract. Two XRD experiments under pressure were recently reported.[23,31] Both investigations made evident that a structural transition toward a cubic phase occurs around 24 GPa (23 ± 2 and 25 GPa, following Refs. 23 and 31, respectively). Optical[22] and electrical resistance[26] experiments seem to indicate a phase transition around 20 GPa. Information about the variation of the **c** axis is available not only from XRD, but also from microphotographies.[19,22] The **c** axis behaves irreversibly if the pressure is increased above 16 ± 2 GPa. Finally, the compressibility of the **a** axis at atmospheric pressure, χ_a, was derived from the elastic constants.[19,24] Due to the van der Waals character of the inter layer interaction, the compressibility of the **c** axis, $\chi_c=24.9\times10^{-3}$ GPa^{-1}, is much larger than the compressibility of the **a** axis; $\chi_a=5\times10^{-3}$ GPa^{-1}.

X-ray-absorption spectroscopy (XAS) is an experimental technique that probes the local environment of the absorbing atom, and consequently complements the long-range order information given by XRD experiments. We have performed high-pressure single-crystal x-ray-absorption spectroscopy at Ga and Se *K* edges up to 34 GPa in order to study the structural evolution of GaSe under pressure. In the sections that follow we shall first of all describe the experimental setup. Afterward, in Sec. III, we will present the inferences drawn from the study of the x-ray-absorption near-edge structure (XANES) part of the spectra, and the details of the extended x-ray-absorption fine-structure (EXAFS) analysis carried out. Then we shall examine the structural changes that occur below 16 ± 2 GPa. Finally we will discuss the value of the structural phase transition pressure obtained with different methods.

II. EXPERIMENT

A wide-angle aperture membrane diamond anvil cell[32] (DAC) was used as the pressure generator. The diamonds were of the Drukker standard type, with a culet size of 0.5 mm. High-quality GaSe crystals were prepared by the Bridgman method. Samples were cleaved from the ingots with a razor blade and cut into parallelepipeds. Single crystal samples of dimensions $100\times150\times30$ μm^3, Ga *K* edge, or $150\times150\times30$ μm^3, Se *K* edge, were placed in a 260- μm-diameter hole drilled in an Inconel gasket. The pressure was measured *in situ* using the linear ruby fluorescence scale.[33]

The x-ray-absorption experiments were carried out at the ID24 energy-dispersive x-ray-absorption station of the European Synchrotron Radiation Facility (Grenoble, France),[34] in two different beamtime allocations.

We performed two different experiments. The first one was performed at the Ga *K* edge (10.368 keV), using silicon oil as pressure transmitting medium. A profiled curved Si(111) monochromator[35] focused the beam to a spot of approximately 50 μm in the horizontal direction. In the vertical direction the beam was only slit down to 100 μm. Details about the principle of energy-dispersive x-ray-absorption data collection can be found elsewhere.[36] The incident intensity I_0 was measured outside the pressure chamber. An essential experimental aspect of XAS experiments in a DAC is the presence of glitches in spectra originated from diffraction peaks of the diamond single crystals. The pressure cell is oriented with respect to the polychromatic x-ray beam in order to remove these glitches from the widest spectral range around the x-ray-absorption edge. This operation takes advantage of the real time visualization of the XAS spectra characteristic of the energy-dispersive setup. Given the geometry of the experiment, the polarization vector of the synchrotron radiation was always in the layer plane.

The second experiment was performed at the Se *K* edge (12.653 keV), using a 4:1 methanol ethanol mixture as pressure transmitting medium, some time after the first. Meanwhile a focusing vertical mirror was installed in ID24. Thanks to the combined action of the new mirror and the previously installed profiled monochromator, the size of the spot at the sample was reduced to 120×60 μm^2. Due to the small size of the focus point and the relative size of the sample and gasket hole, it was possible, for the first time (to the best of our knowledge) in a dispersive XAS experiment, to measure the I_0 through the DAC, close to the sample. As the Se *K* edge is energetically located above the Ga *K* edge, in this second experiment the glitches associated with the diamond diffraction peaks were more numerous and difficult to eliminate from the spectral range of interest. We employed two orientations of the diamond anvil cell. In the first one the XANES part of the spectrum was free of glitches. In the second one there was only one small glitch next to the white line, not affecting the EXAFS part of the spectrum, whose contribution was eliminated by the normalization process.

III. RESULTS AND DISCUSSION

A. XANES

In Fig. 2 we present XANES spectra of GaSe for some pressures. The spectra are taken at the Ga *K* edge [10.368 keV, Fig. 2(a)] and Se *K* edge [12.653 keV, Fig. 2(b)]. The XANES part of the spectra involves photoelectron multiple-scattering paths, and is consequently sensitive to medium range order (up to $\sim$15 Å). XANES can be used as a fingerprint characteristic of the absorbing atom environment to detect structural phase transitions.

In the low pressure spectrum taken at the Se *K* edge the white line shows a doublet structure. The valley separating the two peaks blurs with increasing pressure, and at 16.3

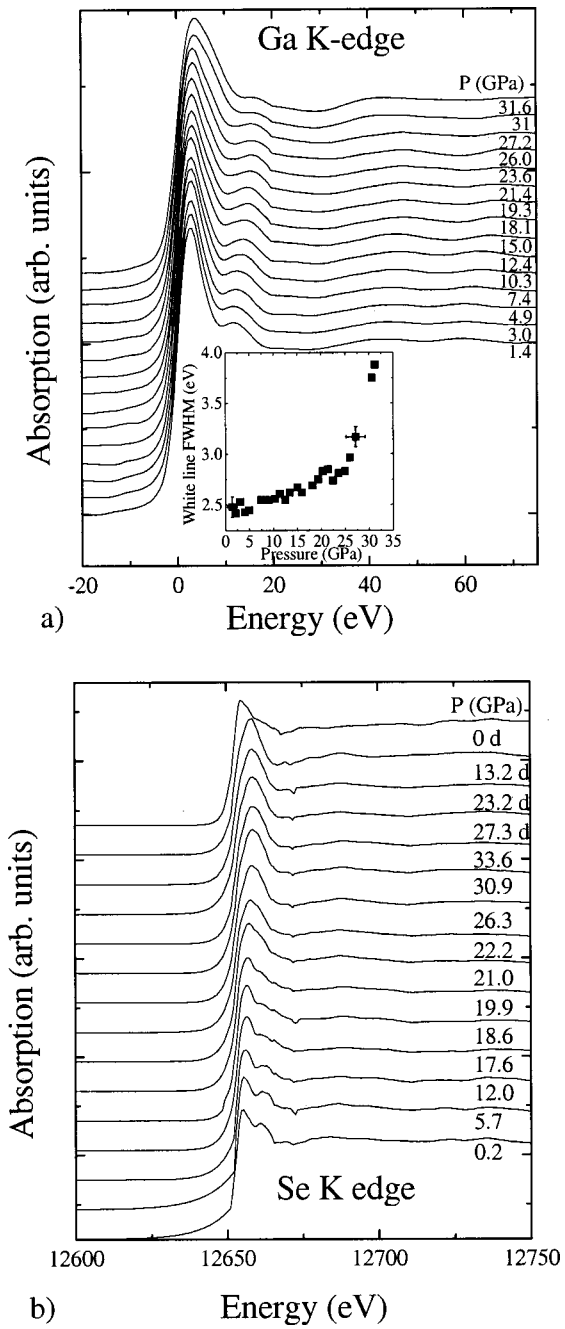

FIG. 2. XANES spectra of GaSe at the Ga *K* edge (a) and the Se *K* edge (b). The numbers next to the spectra refer to the pressure at which the spectra were taken. The letter *d* indicates that the spectra were taken in the downstroke. The inset in (a) represents the white line full width half maximum evolution under pressure.

GPa the second peak has become a shoulder of the first. Then it clearly evolves up to 20 GPa; where the white line has been already transformed into a singlet. We will see later that EXAFS data confirms that these changes observed in the XANES structure correspond to a phase transformation. The same evolution in the white line, from doublet to singlet, has been observed in the Se *K*-edge XANES spectra of InSe during a phase transition from the layered phase to the rock-salt phase.[38] The singlet structure of the white line is maintained in the downstroke up to 13.2 ± 1.5 GPa. The XANES of the recovered sample is different from that of the low- and high-pressure phases. In the spectra taken at the Ga *K* edge, the widening of the white line at 25 ± 3 GPa [see the inset in Fig. 2(a)] can be related to the onset of the structural high-pressure transition.

B. EXAFS

The quality of the spectra in the experiments taken at the Ga *K* edge allows EXAFS analysis up to 400 eV after the edge. We obtained the pseudo-pair-distribution function [(PPDF), Fig. 3(a)] performing a Fourier transform of the EXAFS signal comprised between 3.1 and 10.9 Å^{-1} with a Bessel-type ($\tau=4$) apodization window. The first shell of neighbors is constituted by three Se atoms and one Ga atom, and manifests itself in the PPDF through the maximum extending from approximately 1.4 to 2.8 Å. The Ga atom does not participate in this maximum because the Ga-Ga bond is oriented perpendicularly to the polarization of the incident radiation.

In Fig. 3(a) the amplitude of the maximum corresponding to the first shell of neighbors starts to decrease at 26 ± 3 GPa. At 31 ± 4 GPa there is not any well-defined structure in the PPDF, indicating that the sample is still not completely transformed and that the disorder at this pressure is very high.

At the Se-*K* edge, diamond XRD glitches limited the useful spectral range to 250 eV after the edge. The PPDF was obtained by a Fourier transformation of the EXAFS signal in a *k* domain between 2.7 and 8 Å^{-1}, and using a Bessel based ($\tau=4$) apodization window. It is shown in Fig. 3(b) for some representative pressures. Under ambient conditions the Se environment is constituted by three Ga atoms at 2.47 Å. The contribution of the first-neighbor shell to the PPDF corresponds to the peak observed between approximately 1 and 2.7 Å. The PPDF pattern is not very stable in the low-pressure phase. This instability might be related at least in part to an experimental problem, coming from the influence of residual tails in the x-ray spot. Although the horizontal spatial distribution of the spot is nearly Gaussian, it has low-intensity tails which proved hard to eliminate with different monochomator[35] designs. In the experiment at the Se *K* edge both the I_0 (close to the sample) and I (through the sample) signals were taken through a DAC, and it may be possible that the residual tails in the x-ray spot would have affected the quality of the normalization procedure.

To deduce structural information about the environment of the absorbing atom from EXAFS data, phases and amplitudes have to be known. They are deduced from ambient pressure spectra where all the structural parameters are known,[15] and supposed to be independent of pressure. With the limited spectral range obtained we can not deduce quantitative information from the second maximum of the PPDF because it is originated from the contribution of several atoms situated at distances differing in some tenths of angstroms, and that present distinct behaviors under pressure.

The Ga-Se distance under pressure, as obtained from the EXAFS fit, is depicted in Fig. 4. It is essentially the same for

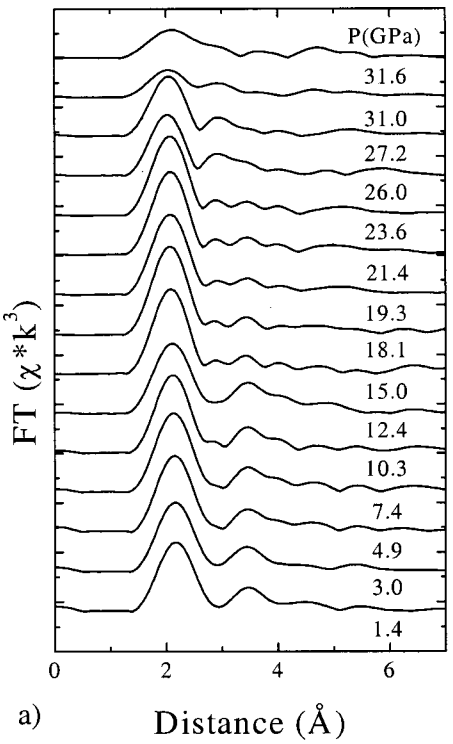

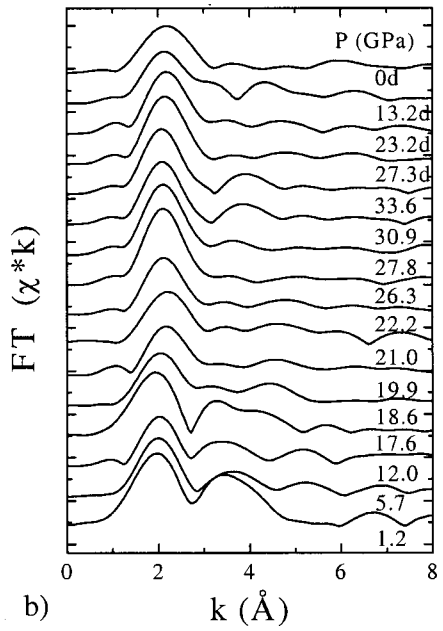

FIG. 3. Pseudo-pair-distribution function (PPDF) obtained by Fourier transformation of the EXAFS signal. (a) Ga *K* edge. The maximum extending between approximately 1.4 and 2.8 Å corresponds to the contribution of the Ga first-neighbor shell to the PPDF. The Ga atom belonging to the first-neighbor shell does not participate in this maximum because the Ga-Ga bond is oriented perpendicularly to the polarization of the incident radiation. (b) Se *K* edge. The three Ga atoms defining the Se first neighbor shell contribute to the PPDF with the maximum extending from 1 to 2.7 Å. The numbers next to the spectra refer to the pressure at which the spectra were taken. The letter *d* indicates if the spectra were taken in the downstroke.

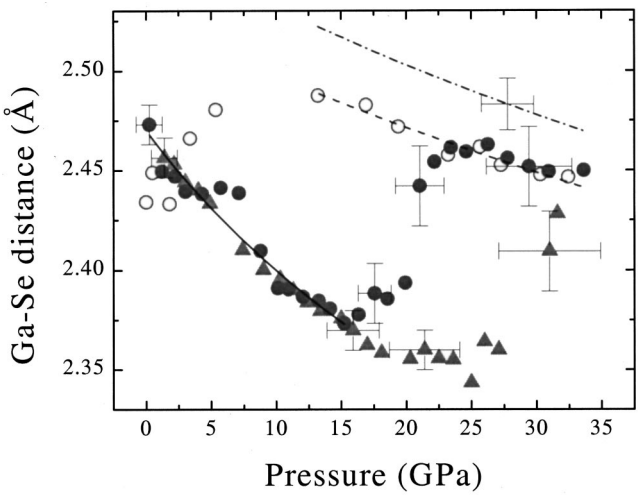

FIG. 4. Ga-Se distance as obtained from the EXAFS fit. (a) Solid triangles: Ga *K* edge, upstroke. (b) Solid circles: Se *K* edge, upstroke. (c) Hollow circles: Se *K* edge: downstroke. (d) Solid line: Murnaghan fit [see Eq. (1)] of (a) and (b) with $d_0 = 2.470 \pm 0.003$ Å, $B_0 = 92 \pm 6$ GPa and B_0' fixed to 5. (e) Dashed line: Murnaghan fit of (c) with $d_0 = 2.53 \pm 0.02$ Å, $B_0 = 260 \pm 40$ GPa, and B_0' fixed to 4.1. (e) Dash-dotted line: Murnaghan fit of data coming from XRD (Ref. 23) with $d_0 = 2.56 \pm 0.01$ Å, $B_0 = 230 \pm 10$ GPa, and B_0' fixed to 4.1.

both experiments up to 15 GPa, although the data coming from the Se *K*-edge experiment present more dispersion. The pressure uncertainties when using either silicon oil or the 4:1 methanol-ethanol mixture as pressure transmitting media have been estimated using the data appearing in Ref. 37, where the dispersion in the pressure measurement given by several ruby grains located at different positions in the pressure chamber is shown. To evaluate the distance error bars we employed the typical uncertainty in EXAFS experiments under pressure, 0.01 Å, established from a comparison of XRD and EXAFS data.[37] In the EXAFS fits concerning the high-pressure phase we continue using the phases and amplitudes of the low-pressure structure, introducing a supplementary error in the determination of the distances. The contribution to the error can be estimated[37] as an additional 0.01 Å, and results in an overall error of 0.02 Å.

We have fitted the monotonous decrease observed up to 15 GPa to a Murnaghan-type equation of state,

$$d_{\mathrm{GaSe}} = d_{\mathrm{GaSe0}} \left(1 + \frac{B_0'}{B_0} P \right)^{-1/3B_0'}, \qquad (1)$$

where d_{GaSe0} is the Ga-Se distance at ambient pressure, B_0 the local isothermal bulk modulus, and B_0' its pressure derivative. The data dispersion and the small pressure range do not allow one to obtain B_0 and B_0' simultaneously. We have fixed B_0' to a value of 5, resulting in a bulk modulus of $B_0 = 92 \pm 6$ GPa. This value is slightly smaller that those found for InSe (116 ± 20 GPa) (Ref. 38) or GaTe (124 ± 6 GPa) (Ref. 39) for the cation-anion distances. The Ga-Se distance deduced from the experiment at the Se *K* edge (solid circles

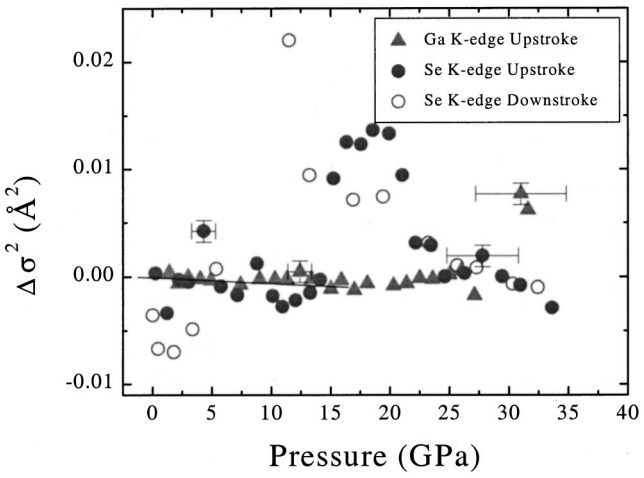

FIG. 5. EXAFS pseudo-Debye-Waller factor variation under pressure as obtained from the EXAFS fit. The line represents a linear fit with slope $(-6\pm6)\times10^{-5}$ Å^2/GPa.

in Fig. 4) shows a high-pressure phase transition at 16 ±2 GPa, in agreement with our XANES conclusions.

The evolution of the Ga-Se distance in the downstroke (hollow circles in Fig. 4) is compatible with the XRD equation of state of the high pressure phase (dash-dotted line) down to around 13 GPa, if we take into account the error in the determination of the distances both in EXAFS and in XRD. A Murnaghan fit (dashed line) to the downstroke points obtained by EXAFS results in $d_0=2.53\pm0.02$ Å and $B_0=260\pm40$ GPa, with B_0' fixed to 4.1. The same fit to the data obtained from XRD gives $d_0=2.56\pm0.01$ Å and $B_0=230\pm10$ GPa with B_0' fixed to 4.1, in agreement with EXAFS results. Below 13 GPa in the downstroke a structural change takes place, and the cation-anion distance obtained tends progressively toward that of hexagonal GaSe.

The EXAFS fit also gives information about static disorder and thermal vibration through the so-called pseudo-Debye-Waller (PDW) factor. In x-ray diffraction the Debye-Waller factor is related to the mean-square deviation in position for each atom. In EXAFS, it is called *pseudo*-Debye-Waller factor because it is related to the deviations in the *relative* position between the absorbing and backscattering atoms. The PDW factor obtained from the EXAFS fit is presented in Fig. 5. Although presenting a considerable dispersion, it diminishes up to 16 ± 2 GPa with a slope of $(-6\pm6)\times10^{-5}$ Å/GPa. The evolution under pressure of the harmonic contribution to the PDW factor can be estimated[37] in the Einstein approximation using the Grüneisen parameter,[19] and the measured decrease in the Ga-Se distance. The result is 8×10^{-4} Å^2, which is of the same order of magnitude than the harmonic contribution to the PDW in GaSe. Therefore, we can conclude that up to 16 ±2 GPa there is no significant increase in the static disorder. In the data taken at the Se *K* edge the PDW increases from 16 ± 2 GPa on, indicating that the static disorder starts to grow. The characteristic disorganization of a phase transition is responsible for the increase in the PDW around 20 GPa. In the downstroke the PDW increases steadily down to 11 GPa, where a structural change brings the PDW to comparable values to that of the low-pressure phase. In the data taken at the Ga *K* edge the PDW starts to increase at 25 ± 3 GPa. This fact will be clarified in Sec. III D.

C. Structural changes up to 15 GPa

We have shown in Sec. III B that up to 15 GPa the Ga-Se distance follows a Murnaghan equation given by $d_{\mathrm{GaSe0}}=2.470\pm0.003$ Å and $B_0=92\pm6$ GPa, with B' fixed to 5. On the other hand, from the x-ray spectra appearing in Ref. 31 it is possible to deduce the evolution under pressure of the **a** axis, resulting in $a_0=3.743\pm0.007$ Å and $B_0=61\pm4$ GPa with B' fixed to 5. The associated compressibility $\chi_a=1/(3B_0)=(5.5\pm0.4)\times10^{-3}$ GPa^{-1} is consistent with the one obtained[19,24] from the elastic constants ($\chi_a=5\times10^{-3}$ GPa^{-1}). From a direct comparison of their associated isothermal bulk modulus it is clear that the Ga-Se distance and the **a** axis do not shrink under pressure at the same rate. To reconcile the two compressibilities, the angle φ between the Ga-Se bond and the plane of the layer (see Fig. 1) should change, as already proposed for InSe (Ref. 38) or GaTe.[39] It seems logical to assume (hypothesis I) that the trigonal axis defined by the Ga-Ga bond remains perpendicular to the layer under compression. Thus the next equation follows:

$$\frac{a}{2}=d_{\mathrm{GaSe}}\cos\varphi\cos 30, \tag{2}$$

As the **a** axis diminishes faster than the GaSe bond length, the angle φ must grow. Concretely, it increases from $29.0\pm0.7°$ at ambient pressure to $30.4\pm0.7°$ at 16 GPa.

GaS is the most symmetric III-VI-layered semiconductor. The atomic arrangement within the unit cell is described by only two independent parameters, and it has been possible[40] to make a complete structural determination using only XRD data. The calculations show that the Ga-Ga and Ga-S bond lengths vary in the same way under pressure. Therefore it is reasonable to suppose (hypothesis II) that in GaSe the Ga-Ga and Ga-Se bond lengths shrink at the same rate under pressure. Assuming only hypotheses I and II, it is possible to give the evolution of the whole structure under pressure:

$$z_{\mathrm{Ga1}}=\frac{1}{2}-z_{\mathrm{Ga2}}, \tag{3}$$

$$z_{\mathrm{Ga2}}=\frac{d_{\mathrm{GaGa}}}{2c}, \tag{4}$$

$$z_{\mathrm{Se1}}=\frac{1}{c}\left(\frac{d_{\mathrm{GaGa}}}{2}+d_{\mathrm{GaSe}}\sin\varphi\right), \tag{5}$$

$$z_{\mathrm{Se2}}=\frac{1}{2}-z_{\mathrm{Se1}}. \tag{6}$$

z_{Ga1}, z_{Ga2}, z_{Se1}, and z_{Se2} are the positional parameters of nonequivalent atoms in the crystallographic unit cell.

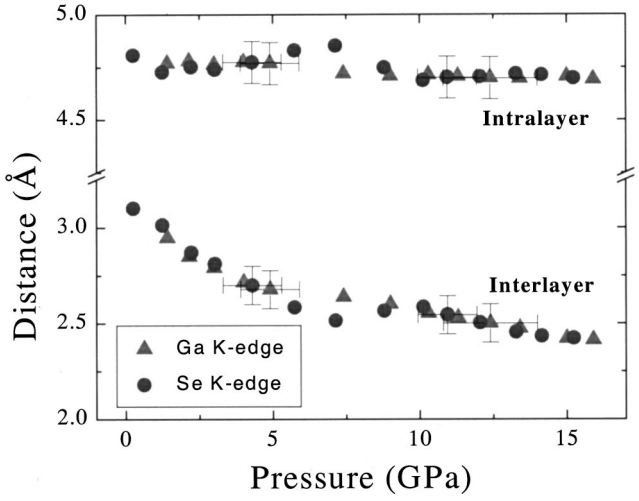

FIG. 6. Evolution of the intralayer and interlayer distances in GaSe.

The intralayer and interlayer distances (see Fig. 1) can be calculated through

$$d_{\text{intralayer}} = d_{\text{GaGa}} + 2d_{\text{GaSe}}\sin(\varphi), \tag{7}$$

$$d_{\text{interlayer}} = \frac{c}{2} - d_{\text{intralayer}}. \tag{8}$$

The resulting variation is represented in Fig. 6. An important conclusion is that the layer compression is not isotropic. Whereas the **a** axis is a 5.2% shorter at 15 GPa than at atmospheric pressure, the intralayer distance shrinks only by 2.4%. In previous works,[19,22,41] before having any indication about the evolution of the internal structure of the layers, they were supposed to follow an isotropic compression under pressure. The dependence of both direct and indirect gaps was directly related to the intralayer and interlayer distances through deformation potentials. Taking into consideration the complex behavior of the structure under pressure, it is clear that the deformation potentials should be reconsidered or at least recalculated. Our structural model was recently introduced in the electronic band calculation of InSe under high pressure.[42]

D. Phase-transition pressure

In our experiment at the Se *K* edge, the Ga-Se distance and PDW augmentations, as well as the XANES change, occur at 16 ± 2 GPa. In the experiment carried out at the Ga *K* edge, the white line and the quality of the EXAFS fits remain unaltered below 25 ± 3 GPa. From that pressure the white line broadens and the Ga-Se distance and the PDW start to grow. The experiment at the Ga *K* edge locates the beginning of the phase transition close to 25 ± 3 GPa, above the value obtained in the Se *K* edge: 16 ± 2 GPa. We think that most of the difference is due to the different pressure transmission media used.

All the experiments on GaSe have been performed under non pure hydrostatic conditions. When the ethanol-methanol mixture is used (this work at the Se *K* edge and Ref. 22), a similar transition pressure is observed (around 16 ± 2 GPa). For other pressure-transmitting media (methanol-ethanol-water,[31] or silicon oil in this work at the Ga *K* edge) a higher pressure is obtained (25 ± 3 GPa). The higher value for the methanol-ethanol-water mixture can be related to its known better hydrostatic properties respect methanol-ethanol alone. Phase transitions in layered compounds are very sensitive to the stress conditions. The difference of transition pressure reflects the difference in the stress induced by the different pressure transmitting media.

As a final remark we can suggest the origin of the destabilization of the layered structure in GaSe. First of all, if the Ga-Ga bond behave as the Ga-Se one up to the structural phase transition, it can be estimated that the interlayer distance between Se atoms at 20 GPa is 3.07 Å. We know that trigonal Se is formed by helical chains of Se atoms.[43] Bonds inside the chains are covalent, whereas the chains are bonded by van der Waals interactions. The covalent bond length is 2.38 Å at ambient pressure and 2.40 Å at 10 GPa.[43,44] The shortest distance between Se atoms of adjacent chains is 3.44 Å at ambient pressure and 2.97 Å at 10 GPa.[44] At 14 GPa trigonal Se is no longer stable.[45,46] Then, from 20 ± 2 GPa on, the interlayer distance in GaSe may be too small for the structure to be stable. The interlayer distance between Se atoms in GaSe is smaller than in InSe (3.4 Å) just before the phase transition, and in this case the destabilization seems to be associated with the weakness of the In-In bond.[38]

IV. CONCLUSIONS

The evolution under pressure of the local structure in GaSe has been studied by XAS experiments at Ga and Se *K* edges up to 34 GPa. Both XANES and EXAFS at the Ga *K*-edge indicate a high-pressure phase transition at 25 ± 3 GPa, in good agreement with diffraction data. The transition pressure at the Se *K* edge is largely affected by the deviatoric stresses in the methanol-ethanol mixture above the freezing point. Nevertheless, this effects allows us to observe the Ga-Se distance in the rocksalt high-pressure phase.

The EXAFS fit of the filtered part of the PPDF corresponding to the first-neighbor shell is used to extract information about the Ga-Se bond length and PDW variation under pressure. The Ga-Se distance follows a monotonic decrease up to 16 ± 2 GPa, that has been fitted with a Murnaghan-type equation of state, giving a value for the local isothermal bulk modulus of $B_0 = 92\pm6$ GPa, with its derivative B_0' fixed to a value of 5. Below 15 ± 1 GPa the DW factor does not show any static disorder induced increase. Assuming that the trigonal symmetry of the Se atoms in the layer plane and the perpendicularity of the Ga-Ga bonds with respect to the layer planes are maintained, and that the Ga-Ga bond length variation is proportional to the Ga-Se one, we have given the evolution of the whole structure under pressure. The most striking consequence of the results is

that the intralayer distance decreases only slightly under pressure. This is due to an increase of the angle between the Ga-Se bond and the layer planes from $29.0 \pm 0.7°$ at ambient conditions to $30.4 \pm 0.7°$ at 15 GPa.

ACKNOWLEDGMENT

This work was partially supported by the Spanish government CICYT under Grant No. MAT95-0391.

*Author to whom correspondence should be addressed. FAX: (34) 6 3983146. Electronic mail: Julio.Pellicer@uv.es

[1] A. Segura, J. P. Guesdon, J. M. Besson, and A. Chevy, J. Appl. Phys. **54**, 876 (1983).
[2] J. Martínez-Pastor, A. Segura, J. L. Valdés, and A. Chevy, J. Appl. Phys. **62**, 1477 (1987).
[3] O. Lang, R. Rudolph, A. Klein, C. Pettenkofer, W. Jaegermann, J. Sánchez, A. Segura, and A. Chevy (unpublished).
[4] Ph. J. Kupecek, H. Le Person, and M. Comte, Infrared Phys. **19**, 263 (1979).
[5] C. Hirlimann, J. F. Morhange, M. A. Kanehisa, A. Chevy, and C. H. Brito Cruz, Appl. Phys. Lett. **55**, 2307 (1989).
[6] K. L. Vodopyanov, L. A. Kulevskii, V. G. Voevodin, A. I. Gribenyukov, K. R. Allakhverduev, and T. A. Kerimov, Opt. Commun. **83**, 322 (1991).
[7] E. Bringuier, A. Bourdon, N. Piccioli, and A. Chevy, Phys. Rev. B **49**, 16 971 (1994).
[8] W. C. Eckhoff, R. S. Putnam, S. Wang, R. F. Curl, and F. K. Tittel, Appl. Phys. B: Lasers Opt. **63**, 437 (1996).
[9] V. K. Lukyanyuk, M. V. Tivarnitskii, and Z. D. Kovalyuk, Phys. Status Solidi A **104**, K41 (1987).
[10] M. Balkanski, C. Julien, and J. Y. Emery, J. Power Sources **26**, 615 (1989).
[11] E. Hatzikraniotis, C. Julien, and M. Balkanski, in *Solid State Batteries*, Vol 101 of *NATO Advanced Study Institute, Series E: Applied Sciences*, edited by C. A. C. Squeira and A. Hooper (Martimes Nijhoff, Dordrecht, 1985), p. 479.
[12] S. Benazeth, Nguyen-Huy Dung, M. Guittard, and P. Laruelle, Acta Crystallogr., Sect. C: Cryst. Struct. Commun. **44**, 234 (1988).
[13] K. Cenzual, L. M. Gelato, M. Penzo, and E. Parthé, Acta Crystallogr., Sect. B: Struct. Sci. **47**, 433 (1991).
[14] W. Schubert, E. Dörre, and M. Kluge, Z. Metallkd. **46**, 216 (1955).
[15] A. Khun, A. Chevy, and R. Chevalier, Phys. Status Solidi A **31**, 469 (1975).
[16] J. C. J. M. Terhell and R. M. A. Lieth, Phys. Status Solidi A **5**, 719 (1971).
[17] F. Jellinek and H. Hahn, Z. Naturforsch. **16**, 713 (1961).
[18] A. Kuhn, R. Chevalier, and A. Rimsky, Acta Crystallogr., Sect. B: Struct. Crystallogr. Cryst. Chem. **31**, 2841 (1975).
[19] M. Gauthier, A. Polian, J. M. Besson, and A. Chevy, Phys. Rev. B **40**, 3837 (1989).
[20] D. Errandonea, F. J. Manjón, J. Pellicer, A. Segura, and V. Muñoz, Phys. Status Solidi B **211**, 33 (1999).
[21] N. Kuroda, O. Ueno, and Y. Nishina, Phys. Soc. Jpn. **55**, 581 (1987).
[22] M. Gauthier, Ph.D. thesis, Université Paris VI, 1984.
[23] U. Schwarz, Ph.D. thesis, University of Darmstadt, 1998.
[24] M. Gatulle, M. Fischer, and A. Chevy, Phys. Status Solidi B **119**, 327 (1983).
[25] D. Errandonea, J. F. Sánchez-Royo, A. Segura, A. Chevy, and L. Roa, High Press. Res. **16**, 13 (1998).
[26] K. J. Dunn and F. P. Bundy, Appl. Phys. Lett. **36**, 709 (1980).
[27] D. Errandonea, Ph.D. thesis, Universidad de Valencia, 1998.
[28] D. Errandonea, A. Segura, V. Muñoz, and A. Chevy, Phys. Status Solidi B **211**, 201 (1999).
[29] D. Errandonea, A. Segura, V. Muñoz, and A. Chevy, Phys. Rev. B **60**, 15 866 (1999).
[30] N. Kuroda, O. Ueno, and Y. Nishina, Phys. Rev. B **35**, 3860 (1987).
[31] M. Takumi, A. Hirata, T. Ueda, Y. Koshio, H. Nishimura, and K. Nagata, Phys. Status Solidi B **223**, 423 (2001).
[32] J. C. Chervin, B. Canny, J. M. Besson, and Ph. Pruzan, Rev. Sci. Instrum. **66**, 2595 (1995).
[33] G. J. Piermarini and S. Block, Rev. Sci. Instrum. **46**, 973 (1975).
[34] M. Hagelstein, A. San Miguel, A. Fontaine, and J. Goulon, J. Phys. IV **7**, 303 (1997).
[35] J. Pellicer-Porres, A. San Miguel, and A. Fontaine, J. Synchrotron Radiat. **5**, 1250 (1998).
[36] H. Tolentino, F. Baudelet, E. Dartyge, A. Fontaine, A. Lena, and G. Tourillon, Nucl. Instrum. Methods Phys. Res. A **286**, 307 (1990).
[37] A. San Miguel, Ph.D. thesis, Université Paris VI, 1993.
[38] J. Pellicer-Porres, A. Segura, A. San Miguel, and V. Muñoz, Phys. Rev. B **60**, 3757 (1999).
[39] J. Pellicer-Porres, A. Segura, A. San Miguel, and V. Muñoz, Phys. Status Solidi B **211**, 389 (1998).
[40] H. d'Amour, W. B. Holzapfel, A. Polian, and A. Chevy, Solid State Commun. **44**, 853 (1982).
[41] A. R. Goñi, A. Cantarero, U. Schwarz, K. Syassen, and A. Chevy, Phys. Rev. B **45**, 4221 (1992).
[42] F. J. Manjón, D. Errandonea, A. Segura, V. Muñoz, G. Tobías, P. Ordejón, and E. Canadell, Phys. Rev. B **63**, 125330 (2001).
[43] R. M. Martin, G. Lucovsky, and K. Heliwell, Phys. Rev. B **13**, 1383 (1976).
[44] K. Tanaka, Phys. Rev. B **42**, 11 245 (1990).
[45] Y. Akahama, M. Kobayashi, and H. Kawamura, Phys. Rev. B **47**, 20 (1993).
[46] Y. Akahama, M. Kobayashi, and H. Kawamura, Phys. Rev. B **56**, 5027 (1997).